SCIENCE CHINA
Chemistry

• ARTICLES •

April 2011 Vol.54 No.4: 617–624
doi: 10.1007/s11426-011-4244-8

Synthesis and properties of copolymers based on 5,6-dinitrobenzothiadiazole with low band gap and broad absorption spectra

WANG Fei, LIU YongSheng, WAN XiangJian, ZHOU JiaoYan & CHEN YongSheng*

Key Laboratory for Functional Polymer Materials and Centre for Nanoscale Science and Technology, Institute of Polymer Chemistry, College of Chemistry, Nankai University, Tianjin 300071, China

Received January 4, 2011; accepted January 24, 2011

One polythiophene derivative PT3T and two low band gap copolymers, PBTT-T3T and PBTT, with different ratios of 5,6-dinitrobenzothiadiazole as the acceptor unit in the polymer backbone have been synthesized by Pd-catalyzed Stille-coupling polymerizations. Thermal stability, X-ray diffraction analyses, UV-vis absorption spectra, photoluminescence spectra and electrochemical properties of the copolymers were investigated. The band gap estimated from UV-vis-NIR spectra of the copolymers films varied from 1.39 to 1.94 eV. Among these copolymers, the films of PBTT-T3T and PBTT, which contain the 5,6-dinitrobenzothiadiazole unit, cover a broad wavelength range in the visible and near-infrared region from 400 to 1000 nm with the maximal peak absorption around 700 nm, which is exactly matched with the maximum in the photon flux of the sun.

copolymer, broad absorption, low band gap, charge transfer

1 Introduction

In the last decade, the design and synthesis of low band gap polymers have attracted a great deal of attention due to their unique optoelectronic properties and their application in organic optoelectronic devices [1–4]. One traditional important spectral region for polymer light emitting diodes is the near-infrared (NIR) regions where the telecommunication frequency windows are located [4–6]. Organic NIR photodetectors using low band gap polymers have tremendous potential in remote control, chemical/biological sensing, optical communication, and spectroscopic and medical instruments [2]. For polymer solar cells, although devices have achieved 8.3% confirmed power conversion efficiencies (PCE) [7], the PCE needs to be further improved before commercialization. One of the main limiting parameters for this is the mismatch of their absorption of the photoactive layer to the solar spectrum. To harvest a larger fraction of the solar photon flux and enhance the PCE in photovoltaic devices, polymers with low band gap that absorb light at the NIR and IR regions of the solar spectrum are needed.

One approach in achieving low band gap conjugated polymers is to alternate the conjugated electron donor (D) unit and conjugated electron acceptor (A) unit along the polymer backbone [8]. By combining an electron donor with an electron acceptor unit, a quinoid mesomeric structure (D–A → D^+=A^-) over the conjugated main chain is formed, and the band gap was reduced significantly. These low band gap polymers are promising candidates for NIR light-emitting materials [4–6] and organic photovoltaic materials [9–11]. Thiophene-based π–conjugated polymers possess extensive π–electron delocalization along the polymer backbone and are well known as good donor materials for solar cells. Benzothiadiazole has been widely used as the acceptor unit in cooperation with varieties of electron-

*Corresponding author (email: yschen99@nankai.edu.cn)

donating units as low band gap donors in bulk heterojunction (BHJ) photovoltaic cells [11–13]. High hole mobility and wide sunlight absorption band could be achieved for the D–A type benzothiadiazole-containing polymers [14]. This category of polymer donors has been extensively studied and has shown outstanding photovoltaic performances. The band gap can be reduced by lowering the LUMO (lowest unoccupied molecular orbital) energy level or/and elevating the HOMO level of the D–A alternating conjugated polymers. It is well known that the LUMO energy levels are mainly determined by the electron acceptors. The more powerful the acceptor, the higher the electron affinity, which finally leads to alower LUMO level in the polymers [15]. 5,6-Dinitrobenzothiadiazole, which contains nitro groups ($-NO_2$), is electron-deficient and thus can serve as an even stronger electron-withdrawing unit than benzothiadiazole, but the copolymers based on this structure are rarely studied [16].

In this work, we report three copolymers with low band gap and broad absorption spectra (Scheme 1) based on thiophene functionalized 5,6-dinitrobenzothiadiazole (BTT) and oligothiophene (T3T) units. The influence of different ratios of BTT units in the polymer backbone on the optical properties is also investigated. Film optical absorption measurement shows that the onset band gaps of these polymers range from 1.39 to 1.94 eV.

2 Experimental

2.1 Materials and reagents

All reactions and manipulations were carried out under argon atmosphere with the use of standard Schlenk techniques. THF was distilled from Na/benzophenone under argon atmosphere. All starting materials were purchased from commercial suppliers and used without further purification. 4,7-Dibromo-5,6-dinitrobenzothiadiazole (**1**) [17], 2-tributylstannyl-4-octyl-thiophene [18], 5,5″-dibromo-3,3″-dioctyl-2,2′:5′,2″-terthiophene (**4**) [19] and 2,5-bis(trimethylstannyl)thiophene (**5**) [20] were prepared according to the literature procedures.

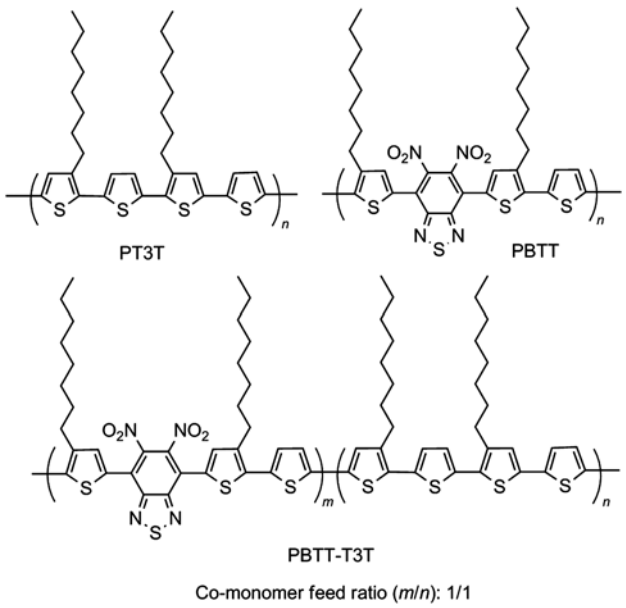

Scheme 1 Chemical structures of the copolymers.

2.2 Instruments and measurements

The ^{1}H NMR spectra were recorded on a Bruker AV400 Spectrometer. Gel permeation chromatography (GPC) analyses were conducted on a Waters 510 system using polystyrene as the standard and THF as eluent at a flow rate of 1.0 mL min^{-1} at 40 °C. Elemental Analyses were performed on an Elementar Vario EL Analyzer. Thermal gravimetric analysis (TGA) and differential scanning calorimetry (DSC) curves were recorded on a NETZSCH STA 409PC instrument under purified nitrogen gas flow with a 5 °C/min heating rate. UV-vis-NIR spectra were obtained with a JASCO V-570 spectrophotometer. Fluorescence spectra were obtained with a FluoroMax-P instrument. X-ray diffraction (XRD) experiments were performed on a Rigaku D/max-2500 X-ray powder diffractometer with Cu-Kα radiation (k = 1.5406 Å) at a generator voltage of 40 kV and a current of 100 mA. Small angle X-ray scattering (SAXS) (Supporting Information) experiments were performed on a Bruker NanoStar SAXS system (Cu Kα radiation source at a voltage of 40 kV and a current of 35 mA). Atomic force microscopy (AFM) studies (Supporting Information) were performed using a Digital Instruments Dimension 3100 microscope in the tapping mode. Cyclic voltammetry (CV) experiments were performed with a LK98B II Microcomputer-based Electrochemical Analyzer. All measurements were carried out at room temperature with a conventional three-electrode configuration employing a glassy carbon electrode as the working electrode, a saturated calomel electrode (SCE) as the reference electrode, and a Pt wire as the counter electrode. CH_3CN was distilled from calcium hydride under dry nitrogen immediately prior to use. Tetrabutylammonium phosphorus hexafluoride (Bu_4NPF_6, 0.1 M) in CH_3CN was used as the supporting electrolyte, and the scan rate was 50 mV s^{-1}. Polymer films were drop-cast onto the glassy-carbon working electrode from chloroform solutions.

2.3 Synthetic procedures

*4,7-Bis-(4-octylthiophen-2-yl)-5,6-dinitrobenzothiadiazole (**2**)* Dichlorobis(triphenylphosphine)-palladium(II) (40 mg, 0.057 mmol) was added to a solution of 4,7-dibromo-5,6-dinitrobenzothiadiazole (**1**) (0.54 g, 1.41 mmol) and 2-tributylstannyl-4-octyl-thiophene (1.94 g, 4.00 mmol) in freshly distilled THF (50 mL) under argon atmosphere. After refluxing for 20 h, the solution was cooled to room tempera-

ture, poured into water (200 mL) and extracted with CH_2Cl_2. The organic layer was thoroughly washed with water, brine and again with water, and then dried over Na_2SO_4. After removal of the solvent, it was chromatographed on silica gel using a mixture of dichloromethane and petroleum ether (1:10) as eluant to afford compound **2** (0.84 g, 98%) as a red solid. ^{1}H NMR (400 MHz, $CHCl_3$): δ (ppm): 7.32 (s, 2H), 7.31 (s, 2H), 2.66 (t, J = 7.7 Hz, 4H), 1.65 (m, J = 7.5 Hz, 4H), 1.28 (m, 20H), 0.88 (t, J = 6.9 Hz, 6H). ^{13}C NMR (100 MHz, $CHCl_3$): δ (ppm): 152.15, 144.38, 141.60, 132.16, 129.21, 126.42, 121.34, 31.87, 30.35, 30.25, 29.40, 29.24, 22.67, 14.12. MALDI-TOF MS: calcd, 614.21; found, 614.23. Anal. calcd for $C_{30}H_{38}N_4O_4S_3$: C, 58.60; H, 6.23; N, 9.11. Found: C, 58.78; H, 6.29; N, 8.82.

*4,7-Bis-(5-bromo-4-octyl-thiophen-2-yl)-5,6-dinitrobenzothiadiazole (**3**)*

N-Bromosuccinimide (1.61 g, 9.04 mmol) was added in small portions to a solution of compound **2** (1.99 g, 3.24 mmol) in chloroform and acetic acid (120 mL, 1/1, *v*/*v*) at 0 °C. After being stirred over night at room temperature, the reaction mixture was poured into water (200 mL) and extracted with CH_2Cl_2. The organic layer was thoroughly washed with water, aqueous sodium bicarbonate, brine and again with water, and then dried over Na_2SO_4. After removal of the solvent it was chromatographed on silica gel using a mixture of dichloromethane and petroleum ether (1:10) as eluant to afford compound **3** (2.12 g, 85%) as a red solid. ^{1}H NMR (400 MHz, $CHCl_3$): δ (ppm): 7.17 (s, 2H), 2.61 (t, J = 7.6 Hz, 4H), 1.60 (m, J = 7.2 Hz, 4H), 1.28 (m, 20H), 0.88 (t, J = 6.6 Hz, 6H). ^{13}C NMR (100 MHz, $CHCl_3$): δ (ppm) 151.68, 143.40, 141.28, 131.64, 129.05, 120.24, 116.89, 31.84, 29.52, 29.40, 29.32, 29.20, 29.09, 22.66, 14.12. MALDI-TOF MS: anal. calcd, 770.03; found, 770.06. Anal. calcd for $C_{30}H_{36}Br_2N_4O_4S_3$: C, 46.64; H, 4.70; Br, 20.68; N, 7.25. Found: C, 46.84; H, 4.80; N, 7.03.

Polymerization of PT3T

Freshly distilled THF (50 mL) was added to the mixture of compound **4** (210 mg, 0.33 mmol), 2,5-bis(trimethylstannyl) thiophene (136 mg, 0.33 mmol) and $Pd(PPh_3)_2Cl_2$ (23 mg, 0.03 mmol) under argon atmosphere. After refluxing for 18 h, the mixture was concentrated and CH_3OH (300 mL) was added, and then the black precipitate was collected on a membrane filter. The polymer was purified by Soxhlet extraction with MeOH, hexane, and chloroform. The chloroform fraction was concentrated and precipitated into methanol to yield the polymer as a dark red solid (64%). GPC (THF): M_n = 12300 g mol^{-1}. ^{1}H NMR(400 MHz, $CDCl_3$): δ (ppm): 7.08 (br, 3H), 7.02 (br, 3H), 2.77 (br, 4H), 1.68 (br, 4H), 1.29 (br, 20H), 0.89 (br, 6H). ^{13}C NMR (100 MHz, $CHCl_3$): δ (ppm): 140.55, 135.97, 135.78, 135.12, 134.93, 134.88, 132.33, 131.70, 129.61, 128.51, 128.12, 126.70, 125.97, 124.38, 31.97, 30.59, 29.75, 29.69, 29.53, 29.36, 22.76, 14.19.

Polymerization of PBTT-T3T

Freshly distilled THF (60 mL) was added to the mixture of compound **3** (160 mg, 0.21 mmol), 2,5-bis(trimethylstannyl) thiophene (172 mg, 0.42 mmol), compound **4** (131 mg, 0.21 mmol) and $Pd(PPh_3)_2Cl_2$ (14 mg, 0.02 mmol) under argon atmosphere. After refluxing for 24 h, the mixture was concentrated and CH_3OH (300 mL) was added, and then the black precipitate was collected on a membrane filter. The polymer was purified by Soxhlet extraction with MeOH, hexane, and chloroform. The chloroform fraction was concentrated and precipitated into methanol to yield the polymer as a black solid (59%). GPC (THF): M_n = 10500 g mol^{-1}. ^{1}H NMR(400 MHz, $CDCl_3$): δ (ppm): 7.29–7.45 (br, 4H), 6.97–7.22 (m, 6H), 2.78 (br, 8H), 1.68 (m, 8H), 1.28 (br, 40H), 0.88 (br, 12H).

Polymerization of PBTT

Freshly distilled THF (50 mL) was added to the mixture of compound **3** (230 mg, 0.30 mmol), 2,5-bis(trimethylstannyl) thiophene (123 mg, 0.30 mmol) and $Pd(PPh_3)_2Cl_2$ (21 mg, 0.03 mmol) under argon atmosphere. After refluxing for 13 h, the mixture was concentrated and CH_3OH (300 mL) was added, and then the black precipitate was collected on a membrane filter. The polymer was purified by Soxhlet extraction with MeOH, hexane, and chloroform. The chloroform fraction was concentrated and precipitated into methanol to yield the polymer as a dark voilet solid (67%). GPC (THF): M_n = 22400 g mol^{-1}. ^{1}H NMR (400 MHz, $CDCl_3$): δ (ppm): 7.54 (br, 1H), 7.37 (br, 3H), 2.86 (m, 4H), 1.70 (m, 4H), 1.28 (br, 20H), 0.88 (m, 6H). ^{13}C NMR (100 MHz, $CHCl_3$): δ (ppm): 151.93, 141.37, 140.88, 137.30, 135.88, 134.04, 133.96, 132.17, 131.60, 128.43, 127.67, 127.45, 124.53, 120.23, 31.88, 30.44, 30.35, 30.26, 29.71, 29.54, 29.45, 29.41, 29.34, 29.29, 29.26, 29.12, 22.68, 14.13.

3 Results and discussion

3.1 Synthesis and thermal stability

The synthesis of the monomers and polymers is depicted in Scheme 2. The starting materials, 4,7-dibromo-5,6-dinitrobenzothiadiazole (**1**) [17], 2-tributylstannyl-4-octyl-thiophene [18], 5,5″-dibromo-3,3″-dioctyl-2,2′:5′,2″-terthiophene (**4**) [19], and 2,5-bis(trimethylstannyl)thiophene (**5**) [20] were synthesized according to the literature. Reaction of compound **1** with 2-tributylstannyl-4-octyl-thiophene using Pd-catalyzed Stille coupling reaction gave compound **2**. Compound **2** was brominated with NBS in $CHCl_3$-AcOH at 0 °C to give the corresponding brominated derivative **3**. The polymers were synthesized according to Pd-catalyzed Stille coupling, using $Pd(PPh_3)_2Cl_2$ as the catalyst and THF as the solvent. The copolymers were purified by continuous

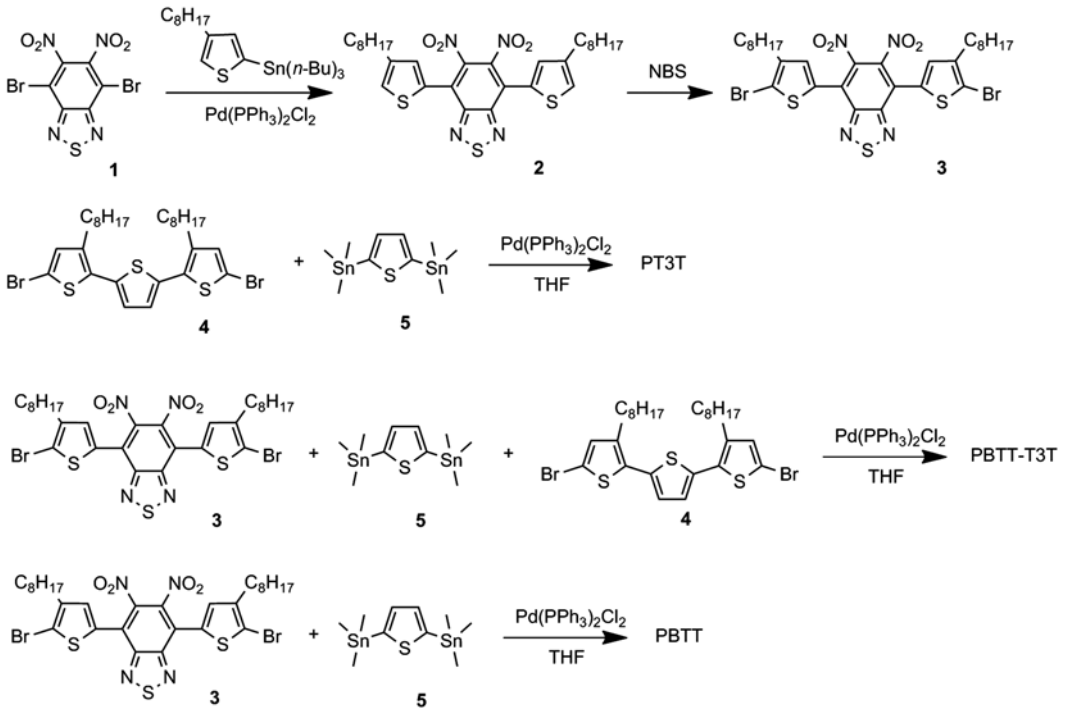

Scheme 2 Synthetic route of the monomers and copolymers.

extraction with methanol, hexane, and chloroform using Soxhlet apparatus. The number-average molecular weights (M_n) of the copolymers were determined by using gel permeation chromatography (GPC) with polystyrene standards in THF. The molecular weight and yield of the copolymers are listed in Table 1. From the ^{1}H NMR spectrum of PBTT-T3T (Figure 1), the molar ratio of m and n is estimated to be 1:1. The synthesized copolymers are readily soluble in organic solvents such as chloroform, tetrahydrofuran (THF) and chlorobenzene.

Thermal properties of the three polymers were investigated by differential scanning calorimetry (DSC) and thermogravimetric analysis (TGA) (Figure 2). As can be seen in Figure 2, no apparent glass transition temperature and melting point was observed, suggesting that these copolymers tend to form amorphous glass state. The onset decomposition temperatures of the polymers at 5% weight loss (T_{5d}) are listed in Table 1. PBTT-T3T and PBTT have their T_{5d} at

Table 1 Molecular weight, 5% weight loss temperature (T_{5d}) and yield of the polymers

Polymer	M_n [a)]	M_w [a)]	PDI	T_{5d} (°C) [b)]	Yield (%)
PT3T	12300	50700	4.12	432	64
PBTT-T3T	10500	14600	1.39	214	59
PBTT	22400	65700	2.93	226	67

a) Number-average molecular weight determined by GPC using polystyrene as the standard in THF solution. b) Decomposition temperature at 5% weight loss determined by TGA in N_2 gas.

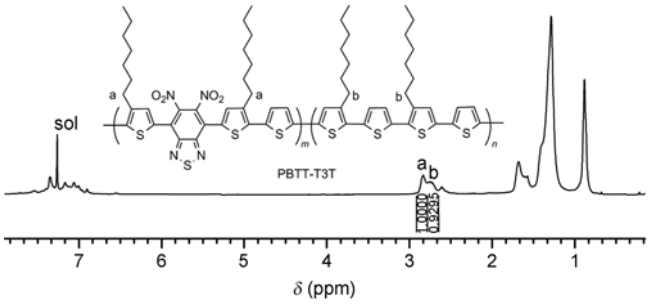

Figure 1 ^{1}H NMR spectrum of the polymer PBTT-T3T.

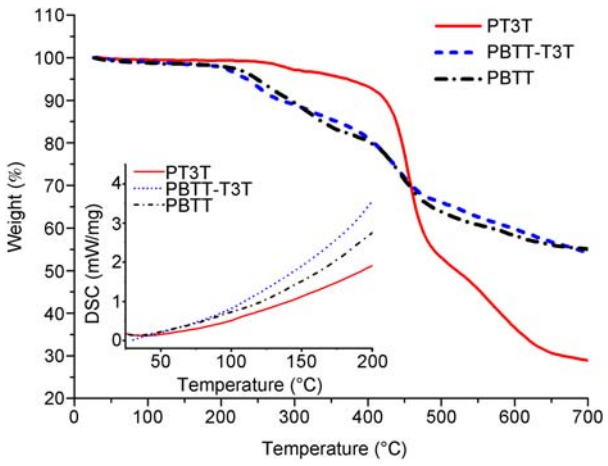

Figure 2 TGA and DSC curves of PT3T, PBTT-T3T and PBTT with a heating rate of 5 °C min^{-1} under N_2.

214 and 226 °C, respectively, while PT3T has the highest onset decomposition temperature at 432 °C. It is apparent that the polymers have good thermal stability for use in organic optoelectronic device.

3.2 X-ray diffraction analyses

To study the crystallinity of these three polymers, X-ray diffraction (XRD) was performed. Figure 3 shows the XRD patterns of powders of PT3T, PBTT-T3T and PBTT. All these three polymers show a broad and weak peak at ~21.2°, corresponding to a *d*-spacing of 4.2 Å. This is believed due to the π-π stacking of the polymer backbone [21]. Since all these polymers were based on 3-octylthiophene, the lattice distances of these polymers were very close to that observed in P3OT (3.8 Å) [22]. It is clear that there is no apparent peak in a small angel region for PT3T, and the peak of PBTT-T3T is not sharp in this region. While polymer PBTT shows a strong and sharp peak around 4.6°, which reveals that the distance between PBTT main chains separated by alkyl side chains is 19.4 Å [21]. This indicates that PBTT has more regular packing at solid state. But overall, the low diffraction intensity of the π-stacking peaks in combination with their broad peaks (between 15° to 35°) suggests that these polymers have rather low crystallinity. Small angle X-ray scattering (SAXS) (Supporting Information) was also performed to study the crystallinity of these polymers, but no sharp reflection peak was observed. So, these polymers mainly show amorphous structure, which is consistent with the DSC results.

3.3 Absorption properties

The UV-vis-NIR absorption properties of the copolymers based on BTT and T3T units are summarized in Table 2. Figure 4(a) shows the UV-vis-NIR absorption in $CHCl_3$ (c = 0.02 mg mL^{-1}). In solution, PT3T has an absorption maximum at 470 nm, which is similar with the absorption spectrum of poly(3-hexylthiophene) (P3HT) [23]. For PBTT-T3T and PBTT, the absorption spectra display two distinct absorption bands. In the absorption spectrum of PBTT, the two absorption peaks are at 374 and 583 nm, respectively. It should be noted that PBTT shows a shoulder peak at ~780 nm, which is a characteristic aggregate absorption [24]. At high concentration, PBTT is partly aggregated in solution and the aggregate increases with the increasing content of the poor solvent when using the mixed solvent (CH_3CN and $CHCl_3$, Supporting Information). Compared with PBTT, the maximum absorption of PBTT-T3T is at 566 nm, and the peak at the low wavelength side is red-shifted to 405 nm by introducing co-monomer T3T units. The absorption peaks of these polymers around 400 nm were attributed to the π-π* transition of the π-conjugated segments in the copolymer backbone, while the peaks at long wavelength band around 570 nm were due to the intramolecular charge transfer between the thiophene donor unit and the 5,6-dinitrobenzothiadiazole acceptor unit [25]. It also can be concluded that the absorption at long wavelength intensifies with the increasing ratio of the electron-withdrawing unit in the copolymer main chain. The optical band gaps of these polymers were approximated by extrapolation of the low-energy edge of each absorption spectrum [26]. From the edge of the absorption spectra (Figure 4(a)), the band gap of the three polymers is estimated to be 1.99, 1.79 and 1.43 eV, respectively. The results show that the optical band gaps decrease with increasing units of the acceptor.

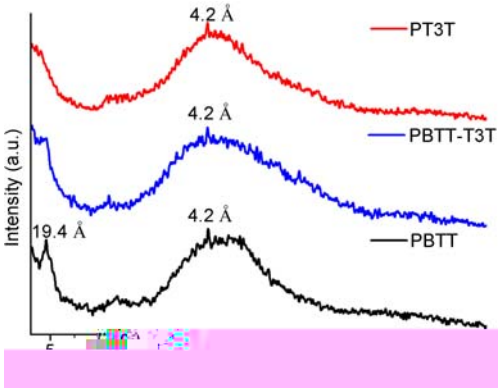

Figure 3 X-ray diffraction patterns of PT3T, PBTT-T3T and PBTT powders. Peaks are labeled with d-spacing in angstroms.

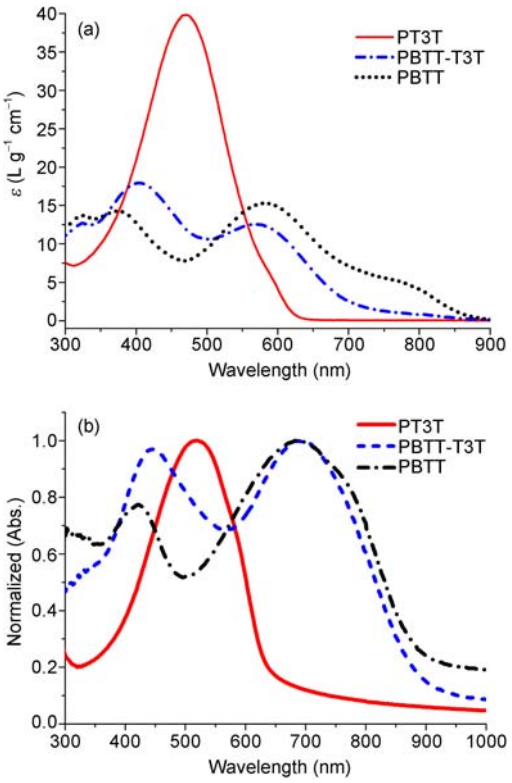

Figure 4 UV–vis-NIR spectra of PT3T, PBTT-T3T and PBTT, (a) 0.02 mg mL^{-1} in $CHCl_3$ and (b) in films.

Thin films of the copolymers were obtained by spin-coating of the corresponding $CHCl_3$ solution onto a glass substrate. Absorption spectra of the thin films (Figure 4(b)) show the similar trends compared to the solution spectra, and in general, a broadening and bathochromic shift of the bands are visible. This broadening and bathochromic shift is strongly induced by the interchain π-π stacking interactions [25]. Compared with solution absorption spectra, the absorption maxima at the long wavelength of films of PT3T, PBTT-T3T and PBTT exhibit a large bathochromic shift, which is 49, 132 and 103 nm, respectively. For PBTT-T3T and PBTT, the absorption band on the low wavelength side also has a bathochromic shift of 43 and 48 nm. As shown in Figure 4(b), the copolymer PBTT-T3T, which was obtained by introducing co-monomer T3T to the copolymer PBTT, has a bathochromic shift of 28 nm for the peak on the low wavelength side compared with that of PBTT. This bathochromic shift may be attributed to the increasing of intramolecular charge transfer from the T3T units to the BTT units, which leads to shifting the absorption spectrum to lower energy. Also, as expected, the copolymer PBTT-T3T has wider and stronger absorption below 550 nm compared with the corresponding mono polymers (PBTT and PT3T), showing both the absorption characteristic of these two mono polymers. In addition, the optical band gaps of PT3T, PBTT-T3T, and PBTT, which were determined from the absorption band edges, lowered to 1.94, 1.40 and 1.39 eV, respectively. It is noteworthy that the absorption spectra of PBTT-T3T and PBTT cover a broad wavelength range in the visible and NIR region from 400 nm to 1000 nm with the maximal peak absorption around 700 nm, which matches with the maximum in the photon flux of the sun [9].

3.4 Electrochemical properties

To investigate the electrochemical properties of these copolymers and estimate their band gap, we performed cyclic voltammetry (CV) measurements on films of the polymers under argon atmosphere. Polymer films were drop-cast onto the glassy-carbon working electrode from chloroform solutions. Cyclic voltammetry of all copolymers in anhydrous acetonitrile in the presence of Bu_4NPF_6 as supporting electrolyte at a scan rate of 50 mV s^{-1} is shown in Figure 5, and all the electrochemical data are summarized in Table 3. As shown in Figure 5, PT3T displays a partly reversible oxidation process, PBTT-T3T and PBTT display irreversible oxidation waves and no clear reduction waves were detected for all these copolymers. The HOMO (highest occupied molecular orbital) energy levels of the copolymers were calculated using the following empirical equation: $E_{HOMO} = -e(E^{ox}_{onset} + 4.4)$ (eV), where E^{ox}_{onset} is the onset oxidation potential versus standard calomel electrode (SCE). Because the onset reduction potentials of PBTT-T3T and PBTT were not observed clearly during the reduction measurement process, the LUMO energy levels of these polymers were calculated from the HOMO levels and optical band gap (E^{opt}_g): $E_{LUMO} = E^{opt}_g + E_{HOMO}$ (eV). The onset oxidation potential (E^{ox}_{onset}) of PT3T, PBTT-T3T and PBTT is 0.77, 1.12 and 1.19 eV, respectively. The E^{opt}_g (1.94 eV), HOMO (–5.17 eV), and LUMO (–3.23 eV) of PT3T are almost identical to those of regioregular P3HT (1.9, –5.1, and –3.2 eV, respectively) reported in the literature [27], since the structure of PT3T is similar to that of P3HT. The HOMO level of PBTT is –5.59 eV, which is 0.07 eV lower than that of PBTT-T3T. The higher content of strong electron-withdrawing effect of 5,6-dinitrobenzothiadiazole in PBTT backbone is the main reason for the lower HOMO level of PBTT. As we indicated earlier, we did not observe any clear reduction peak for polymer PBTT-T3T and PBTT. This may attribute to the surrounding effect of thiophenes flock [16, 28]. The E_{LUMO} values of PBTT-T3T and PBTT, which are determined from the differences between HOMO energy levels and optical band gaps, are –4.12 eV for PBTT-T3T and –4.20 eV for PBTT, respectively. Here, the LUMO energy levels of PBTT-T3T and PBTT are lower than that

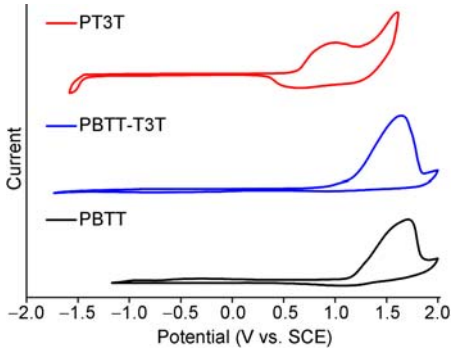

Figure 5 Cyclic voltammetry of the films of PT3T, PBTT-T3T and PBTT on a glassy carbon electrode in CH_3CN with 0.1 M Bu_4NPF_6 as supporting electrolyte and a scan speed of 50 mV s^{-1}.

Table 2 Photophysical properties of PT3T, PBTT-T3T and PBTT

Polymer	Solution [a]	Thin film	Optical band gap	
	λ_{max}^{abs} (nm) (ε_{max}, L g^{-1} cm^{-1})	λ_{max}^{abs} (nm)	Solution [a] (eV)	Film (eV)
PT3T	470 (39.83)	519	1.99	1.94
PBTT-T3T	405 (17.93); 566 (12.55)	448; 698	1.79	1.40
PBTT	374 (14.28); 583 (15.29)	422; 686	1.43	1.39

a) Measured in $CHCl_3$ (ρ = 0.02 mg mL^{-1}).

Table 3 Redox properties of PT3T, PBTT-T3T and PBTT

Polymer	E^{ox}_{onset} (V)	HOMO (eV)	LUMO (eV) [a]
PT3T	0.77	–5.17	–3.23
PBTT-T3T	1.12	–5.52	–4.12
PBTT	1.19	–5.59	–4.20

a) $E_{LUMO} = E^{opt}_g + E_{HOMO}$.

of PCBM (E_{LUMO} = −3.8 eV) [29], which is widely used as the electron acceptor in polymer solar cells. So, PBTT-T3T and PBTT might be used as the polymer electron acceptor. We have done a preliminary screening for the photovoltaic devices using P3HT as the donor and PBTT-T3T or PBTT as acceptor, but the power conversion efficiencies were very low (~0.01%). We used the atomic force microscopy (AFM) to investigate the morphology of the blend film (Supporting Information), and no desired phase separation for an efficient OPV active layer was observed. Also, a matching hole transport polymer as the donor which could better match these polymers may be needed to have high photovoltaic performance [30–32].

3.5 Photoluminescence characteristics

Photoluminescence (PL) spectra for the copolymers were taken under an excitation of 467 nm in 0.01 mg mL^{-1} chloroform solutions (Figure 6(a)). The emission curves of PT3T, PBTT-T3T and PBTT show their emission maxima at 572, 559 and 569 nm, respectively. The intensity of the PL emission decreases by introducing BTT content into the copolymer backbone. The emission peak was mostly quenched for PBTT-T3T, especially for PBTT. This result is consistent with the expected intramolecular charge transfer from the thiophene donor to the 5,6-dinitrobenzothiadiazole acceptor [33].

The PL spectra of PT3T, PBTT-T3T and PBTT in solid films (spin-coated from dichlorobenzene solutions, 10 mg mL^{-1}) excited at 524, 447 and 422 nm, respectively, are shown in Figure 6(b). Compared with their solution PL spectra, the emission maximum of PT3T, located at 619 nm, exhibits a large bathochromic shift of 47 nm. The bathochromic shift of the PL peak could be attributed to the increase of effective conjugation length and the interchain interactions of PT3T at solid state [34], which is also supported by XRD analysis. Interestingly, the PL spectra of copolymers PBTT-T3T and PBTT containing BTT moieties in Figure 6(b) were completely quenched in solid films. An additional reason for the complete PL quenching phenomena of these polymers should be the normal intermolecular energy transfer at solid state in the films.

To get an insight into the charge transfer process in the donor/acceptor blends, the PL spectra of P3HT/PBTT-T3T and P3HT/PBTT blends along with that of the pure P3HT spin-coated films from dichlorobenzene solutions have been investigated. As shown in Figure 7, the PL of P3HT film locates in the visible-NIR region with an emission maximum at 724 nm, and is completely quenched after blending with the acceptor polymer PBTT-T3T or PBTT. This observation indicates that an efficient charge/energy transfer occurred between the P3HT and the acceptor polymers and these two polymers may be used as the electron acceptor in OPV devices.

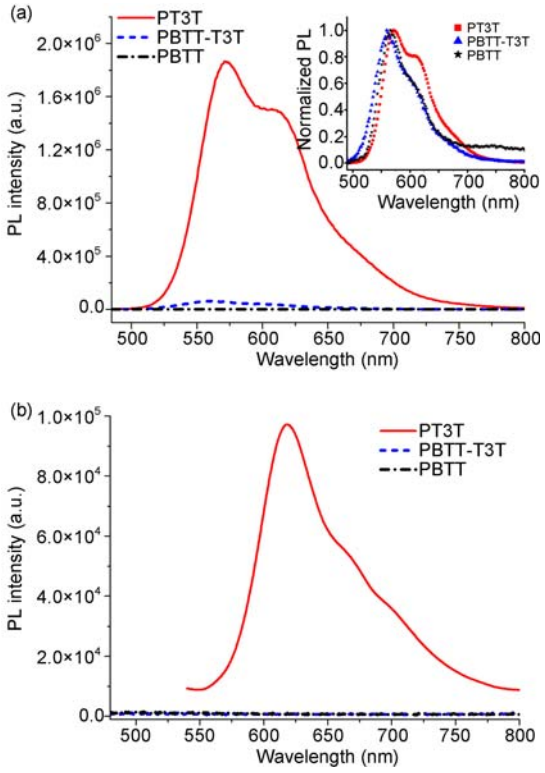

Figure 6 Photoluminescence spectra of PT3T, PBTT-T3T and PBTT: (a) 0.01 mg mL^{-1} in $CHCl_3$ solutions and (b) solid films (spin-coated from ODCB solutions). The inset shows the normalized PL spectra.

4 Conclusions

We have synthesized one polythiophene derivative PT3T and two low band gap copolymers based on thiophene functionalized 5,6-dinitrobenzothiadiazole units and oligothiophene units by Pd-catalyzed Stille-coupling polymerizations. The polymers, PBTT-T3T and PBTT, show a broad absorption spectrum from 400 to 1000 nm. With increasing ratio of electron-withdrawing unit 5,6-dinitrobenzothiadiazole in the polymer backbone, the band gaps of the polymers

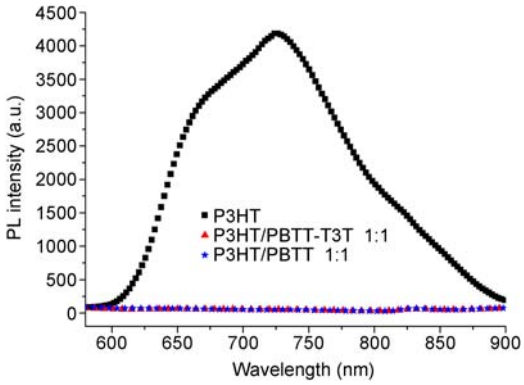

Figure 7 Photoluminescence spectra of P3HT/PBTT-T3T, P3HT/PBTT blend films with weight ratio of 1:1 and the pure P3HT film upon excitation at 553 nm. The films were spin-coated on quartz from dichlorobenzene solution.

decrease. Among these three polymers, PBTT shows the smallest band gap of 1.39 eV. Complete PL quenching was observed when P3HT blended with PBTT-T3T or PBTT, indicating efficient charge/energy transfer occurred. The low band gap, broad absorption spectra, coupled with their good solubility and stability, indicate that PBTT and PBTT-T3T could be used in organic optoelectronic devices such as polymer solar cells and NIR detectors. But initial screening test using PBTT-T3T and PBTT as the electron acceptor for OPV devices gives rather poor power conversion efficiencies. Further optimization is currently underway for their applications.

The authors gratefully acknowledge the financial support from the National Natural Science Foundation of China (50933003 & 50903044) and MOST of China (2009AA032304).

1 Zhang X, Steckler TT, Dasari RR, Ohira S, Potscavage WJ, Tiwari SP, Coppee S, Ellinger S, Barlow S, Bredas JL, Kippelen B, Reynolds JR, Marder SR. Dithienopyrrole-based donor-acceptor copolymers: Low band-gap materials for charge transport, photovoltaics and electrochromism. *J Mater Chem*, 2010, 20: 123–134
2 Yao Y, Liang YY, Shrotriya V, Xiao SQ, Yu LP, Yang Y. Plastic near-infrared photodetectors utilizing low band gap polymer. *Adv Mater*, 2007, 19: 3979–3983
3 Wienk MM, Turbiez M, Gilot J, Janssen RAJ. Narrow-bandgap diketo-pyrrolo-pyrrole polymer solar cells: The effect of processing on the performance. *Adv Mater*, 2008, 20: 2556–2560
4 Thompson BC, Madrigal LG, Pinto MR, Kang TS, Schanze KS, Reynolds JR. Donor-acceotor copolymers for red- and near-infrared-emitting polymer light-emitting diodes. *J Polym Sci, Part A: Polym Chem*, 2005, 43: 1417–1431
5 Brabec CJ, Winder C, Sariciftci NS, Hummelen JC, Dhanabalan A, van Hal PA, Janssen RAJ. A low-bandgap semiconducting polymer for photovoltaic devices and infrared emitting diodes. *Adv Funct Mater*, 2002, 12: 709–712
6 Qian G, Zhong Z, Luo M, Yu DB, Zhang ZQ, Wang ZY, Ma DG. Simple and efficient near-infrared organic chromophores for light-emitting diodes with single electroluminescent emission above 1000 nm. *Adv Mater*, 2009, 21: 111–116
7 http://www. konarka. com.
8 Kitamura C, Tanaka S, Yamashita Y. Design of narrow-bandgap polymers. Syntheses and properties of monomers and polymers containing aromatic-donor and *o*-quinoid-acceptor units. *Chem Mater*, 1996, 8: 570–578
9 Winder C, Sariciftci NS. Low bandgap polymers for photon harvesting in bulk heterojunction solar cells. *J Mater Chem*, 2004, 14: 1077–1086
10 Colladet K, Fourier S, Cleij TJ, Lutsen L, Gelan J, Vanderzande D, Nguyen LH, Neugebauer H, Sariciftci S, Aguirre A, Janssen G, Goovaerts E. Low band gap donor-acceptor conjugated polymers toward organic solar cells applications. *Macromolecules*, 2007, 40: 65–72
11 Blouin N, Michaud A, Leclerc M. A low-bandgap poly(2,7-carbazole) derivative for use in high-performance solar cells. *Adv Mater*, 2007, 19: 2295–2300
12 Yue W, Zhao Y, Shao SY, Tian HK, Xie ZY, Geng YH, Wang FS. Novel NIR-absorbing conjugated polymers for efficient polymer solar cells: effect of alkyl chain length on device performance. *J Mater Chem*, 2009, 19: 2199–2206
13 Park SH, Roy A, Beaupre S, Cho S, Coates N, Moon JS, Moses D, Leclerc M, Lee K, Heeger AJ. Bulk heterojunction solar cells with internal quantum efficiency approaching 100%. *Nat Photonics*, 2009, 3: 297–303
14 Chen JW, Cao Y. Development of novel conjugated donor polymers for high-efficiency bulk-heterojunction photovoltaic devices. *Acc Chem Res*, 2009, 42: 1709–1718
15 Chen CH, Hsieh CH, Dubosc M, Cheng YJ, Su CS. Synthesis and characterization of bridged bithiophene-based conjugated polymers for photovoltaic applications: Acceptor strength and ternary blends. *Macromolecules*, 2010, 43: 697–708
16 He YJ, Wang X, Zhang J, Li YF. Low bandgap polymers by copolymerization of thiophene with benzothiadiazole. *Macromol Rapid Commun*, 2009, 30: 45–51
17 Perzon E, Wang XJ, Admassie S, Inganas O, Andersson MR. An alternating low band-gap polyfluorene for optoelectronic devices. *Polymer*, 2006, 47: 4261–4268
18 Voituriez A, Mellah M, Schulz E. Design and electropolymerization of new chiral thiophene-salen complexes. *Synth Met*, 2006, 156: 166–175
19 Liu YS, Zhou JY, Wan XJ, Chen YS. Synthesis and properties of acceptor-donor-acceptor molecules based on oligothiophenes with tunable and low band gap. *Tetrahedron*, 2009, 65: 5209–5215
20 Van Pham C, Macomber RS, Mark HB, Jr Zimmer H. Lithiation reaction of 2,5-dibromothiophene. Carbon-13 NMR spectra of 3-substituted derivatives. *J Org Chem*, 1984, 49: 5250–5253
21 Blouin N, Michaud A, Gendron D, Wakim S, Blair E, Neagu-Plesu R, Belletete M, Durocher G, Tao Y, Leclerc M. Toward a rational design of poly(2,7-carbazole) derivatives for solar cells. *J Am Chem Soc*, 2007, 130: 732–742
22 Samitsu S, Shimomura T, Heike S, Hashizume T, Ito K. Effective production of poly(3-alkylthiophene) nanofibers by means of Whisker method using anisole solvent: Structural, optical, and electrical properties. *Macromolecules*, 2008, 41: 8000–8010
23 Shrotriya V, Ouyang J, Tseng RJ, Li G, Yang Y. Absorption spectra modification in poly(3-hexylthiophene): Methanofullerene blend thin films. *Chem Phys Lett*, 2005, 411: 138–143
24 Li LG, Tang HW, Wu HX, Lu GH, Yang XN. Effects of fullerene solubility on the crystallization of poly(3-hexylthiophene) and performance of photovoltaic devices. *Org Electron*, 2009, 10: 1334–1344
25 Biniek L, Chochos CL, Leclerc N, Hadziioannou G, Kallitsis JK, Bechara R, Leveque P, Heiser T. A [3,2-b]thienothiophene-alt-benzothiadiazole copolymer for photovoltaic applications: Design, synthesis, material characterization and device performances. *J Mater Chem*, 2009, 19: 4946–4951
26 Cao J, Kampf JW, Curtis MD. Synthesis and characterization of bis (3,4-ethylene-dioxythiophene)-(4,4′-dialkyl-2,2′-bithiazole) co-oligomers for electronic applications. *Chem Mater*, 2003, 15: 404–411
27 Kim JY, Lee K, Coates NE, Moses D, Nguyen TQ, Dante M, Heeger AJ. Efficient tandem polymer solar cells fabricated by all-solution processing. *Science*, 2007, 317: 222–225
28 Li K, Qu JL, Xu B, Zhou YH, Liu LJ, Peng P, Tian WJ. Synthesis and photovoltaic properties of novel solution-processable triphenylamine-based dendrimers with sulfonyldibenzene cores. *New J Chem*, 2009, 33: 2120–2127
29 Hellstrom S, Zhang FL, Inganas O, Andersson MR. Structure-property relationships of small bandgap conjugated polymers for solar cells. *Dalton Trans*, 2009, 45: 10032–10039
30 Holcombe TW, Woo CH, Kavulak DFJ, Thompson BC, Frechet JMJ. All-polymer photovoltaic devices of poly(3-(4-*n*-octyl)-phenylthiophene) from Grignard Metathesis (GRIM) polymerization. *J Am Chem Soc*, 2009, 131: 14160–14161
31 Koetse MM, Sweelssen J, Hoekerd KT, Schoo HFM, Veenstra SC, Kroon JM, Yang XN, Loos J. Efficient polymer: Polymer bulk heterojunction solar cells. *Appl Phys Lett*, 2006, 88: 083504
32 Sang GY, Zou YP, Huang Y, Zhao GJ, Yang Y, Li YF. All-polymer solar cells based on a blend of poly[3-(10-*n*-octyl-3-phenothiazinevinylene)thiophene-*co*-2,5-thiophene] and poly[1,4-dioctyloxyl-*p*-2,5-dicyanophenylenevinylene]. *Appl Phys Lett*, 2009, 94: 193302
33 Xia YJ, Luo J, Deng XY, Li XZ, Li DY, Zhu XH, Yang W, Cao Y. Novel random low-band-gap fluorene-based copolymers for deep red/near infrared light-emitting diodes and bulk heterojunction photovoltaic cells. *Macromol Chem Phys*, 2006, 207: 511–520
34 Samuel IDW, Rumbles G, Collison CJ. Efficient interchain photoluminescence in a high-electron-affinity conjugated polymer. *Phys Rev B*, 1995, 52: 11573–11576